An overview of (selected) recent results in finite-temperature lattice QCD

Alexei Bazavov

Physics Department, Brookhaven National Laboratory, Upton, NY 11973, USA

E-mail: obazavov@quark.phy.bnl.gov

Abstract. I discuss recent results on the lattice with the main emphasis on the thermodynamics of the crossover region, restoration of the chiral symmetry and fluctuations of conserved charges as an indicator of deconfinement, that may also be used to determine the chemical freeze-out conditions in heavy-ion collision experiments.

1. Introduction

It has been established by lattice QCD calculations that at the physical values of light quark masses and at vanishing chemical potential there is no genuine phase transition in QCD, but rather an analytic crossover [1, 2, 3]. While the low-temperature phase exhibits confinement and breaking of the chiral symmetry, at high temperatures the behavior of the theory is qualitatively different – the interaction between quarks and gluons decreases due to the asymptotic freedom, leading to deconfinement, and the chiral symmetry is restored (see [4] for a recent review). At the crossover the QCD partition function does not exhibit a singularity, so it is not a surprise that different physical observables show a change in the their temperature dependence at somewhat different temperatures.

2. Restoration of chiral symmetry and T_{pc} in QCD

Let us start the discussion with the phenomena of restoration of chiral symmetry. The QCD Lagrangian at zero light quark mass allows for independent left and right rotations, *i.e.* possesses $SU(2)_L \times SU(2)_R$ symmetry. This symmetry is however spontaneously broken by the vacuum, as indicated by condensate of quark anti-quark pairs. It is expected on general grounds [5] that at zero light quark mass there is a second-order phase transition in QCD (in the $O(4)$ universality class) for which the chiral condensate is the order parameter. The renormalized quark condensate Δ_{ls} (I reserve the name "chiral condensate" for the light quark condensate at zero mass) is shown in Fig. 1 and defined as:

$$\Delta_{ls} = \frac{\langle\bar{\psi}_l\psi_l\rangle_T - \frac{m_l}{m_s}\langle\bar{\psi}_s\psi_s\rangle_T}{\langle\bar{\psi}_l\psi_l\rangle_0 - \frac{m_l}{m_s}\langle\bar{\psi}_s\psi_s\rangle_0}, \quad \langle\bar{\psi}_q\psi_q\rangle = \frac{T}{V}\frac{\partial \ln Z}{\partial m_q} = \frac{1}{N_s^3 N_\tau}\left\langle \mathrm{Tr} M_q^{-1}\right\rangle, \quad q = l, s, \tag{1}$$

where M_q is the fermion matrix, *i.e.* the discretized version of the Dirac operator, $N_s^3 N_\tau$ is the four-dimensional lattice volume. The disconnected susceptibility which is proportional to

fluctuations of the quark condensate

$$\chi_l^{disc} = \frac{1}{N_s^3 N_\tau} \left\{ \left\langle \left(\mathrm{Tr} M_l^{-1} \right)^2 \right\rangle - \left\langle \mathrm{Tr} M_l^{-1} \right\rangle^2 \right\} \tag{2}$$

is shown in Fig. 2. The results are with the asqtad and HISQ/tree action at the light quark mass $m_l = m_s/20$ (somewhat heavier but close to the physical $m_l = m_s/27$).

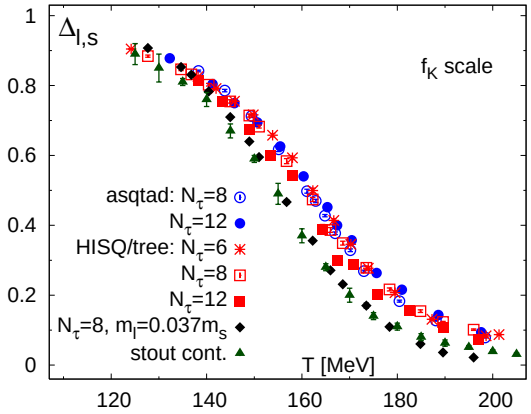

Figure 1. The renormalized quark condensate with the asqtad and HISQ/tree action.

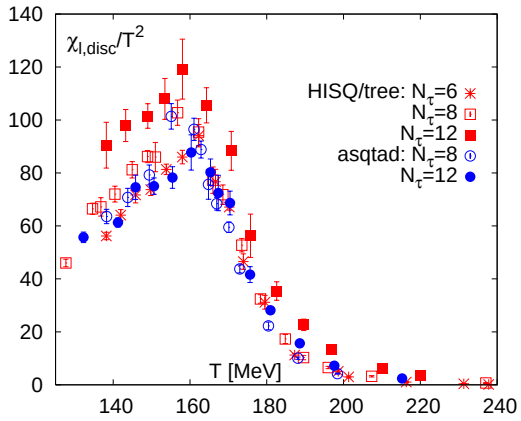

Figure 2. The disconnected susceptibility with the asqtad and HISQ/tree action.

If the physical light quark mass is small enough one may hope that remnants of criticality (plus subleading corrections) still govern the crossover region. Applicability of the critical scaling was extensively studied in Ref. [6] with staggered fermions and the scaling was indeed observed. (An additional complication for staggered fermions is that at non-zero lattice spacing the relevant universality class is $O(2)$ rather than $O(4)$. Luckily, the numerical difference between $O(2)$ and $O(4)$ fits is not significant for our discussion, comparable with other uncertainties, and we refer to this analysis as $O(N)$ scaling.) This approach has been taken by the HotQCD collaboration, who calculated the light quark condensate and its susceptibility with the asqtad and HISQ/tree actions on lattices with the temporal extent $N_\tau = 6$, 8 and 12 at several values of the light quark mass and then performed fits to $O(N)$ scaling functions complemented by non-singular terms. The pseudo-critical temperature, T_{pc}, defined this way as a location of the peak of the chiral susceptibility, reduces to the true critical temperature in the chiral limit. The result in the continuum limit at the physical light quark mass is $T_{pc} = 154(9)$ MeV [7]. This is compatible with the earlier results by the Budapest-Wuppertal collaboration that are in a range $T_{pc} = 147 - 157$ MeV, depending on what chiral observable is picked to determine T_{pc} [8].

The studies discussed so far rely on staggered fermions (one of the numerically cheapest lattice fermion formulations). The fermion doubling problem leads to 16 species of lattice fermions per one in continuum and staggered fermions reduce them to 4 species. The latter are however non-degenerate (and are labeled by "taste" to distinguish from flavor). In other words, taste symmetry is broken, for particular actions we use at $O(a^2)$, a being the lattice spacing. This leads to distorted hadron spectrum, and taste-breaking effects have been identified as the largest source of systematic errors in staggered simulations (a discussion in relation to thermodynamics is presented in Ref. [9]). It is desirable to have independent tests of the results also with other types of lattice fermions. The latter require more computational resources so calculations directly at the physical mass may not be feasible. However, some conclusions can be drawn from simulations at heavier masses. The Budapest-Wuppertal collaboration showed agreement between the continuum-extrapolated light quark condensate for staggered and Wilson

fermions at the pion mass $m_\pi = 545$ MeV [10], Fig. 3 (left). Another study by the same group compared the condensate with overlap fermions (that provide exact chiral symmetry at non-zero lattice spacing) again to staggered at $m_\pi = 350$ MeV [11]. Although the continuum limit for overlap has not been taken, it seems, Fig. 3 (middle), that disagreement would be unlikely. The HotQCD collaboration pursued simulations with domain-wall fermions at $m_\pi = 200$ MeV [12]. A comparison of the staggered and domain-wall disconnected chiral susceptibility is shown in Fig. 3 (right). Note similar location of the peak in the domain-wall (DWF) and HISQ/tree $N_\tau = 12$ data. (Strictly speaking, results for different lattice actions should be compared in the continuum limit, however, Fig. 3 (right) provides a very encouraging check.)

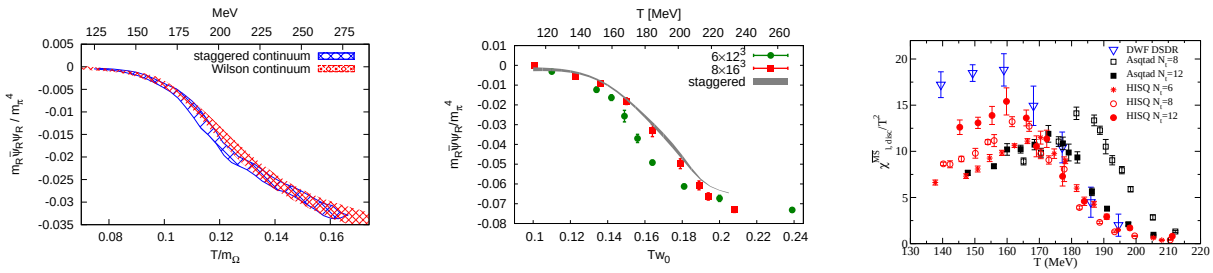

Figure 3. Comparison of the observables indicating restoration of the chiral symmetry between staggered and three other fermion formulations (Wilson, overlap and domain-wall). See text for details.

3. Deconfinement and fluctuations of conserved charges

QCD with infinitely heavy quarks, *i.e.*, $SU(3)$ pure gauge theory, exhibits first-order phase transition at $T_c \simeq 260$ MeV [13]. The order parameter is the renormalized Polyakov loop:

$$L_{ren}(T) = \exp(-cN_\tau/2) \left\langle \frac{1}{3}\mathrm{Tr} \prod_{x_0=1}^{N_\tau} U_0(x_0, \vec{x}) \right\rangle, \qquad (3)$$

where $U_0(x_0, \vec{x})$ is the gauge field in the time direction. The exponential prefactor takes care of the multiplicative renormalization. L_{ren} can be related to the free energy of a static test quark $F_Q(T)$ as $L_{ren}(T) = \exp(-F_Q/T)$. In pure gauge theory the Svetitsky-Yaffe argument [14] allows to interpret deconfinement as a transition from the symmetric phase, $L_{ren} = 0$, into the broken phase, $L_{ren} \neq 0$, where the Polyakov assumes one of the three equally possible values, related by Z_3 symmetry. So, historically, based on the experience from pure gauge theory, the Polyakov loop served as an indicator of deconfinement in lattice QCD. Dialing quark masses to smaller values breaks the Z_3 symmetry (making one of the values of L_{ren} preferable over others, just like a magnetic field in spin systems). Due to string breaking by light dynamical quarks in QCD the value of L_{ren} is always non-zero in the confined phase. Thus, in QCD the Polyakov loop loses its meaning of the order parameter and is not related to any singularity of the partition function (in the chiral limit). As one can see in Fig. 4 (left) the temperature dependence of the Polyakov loop in $SU(2)$ and $SU(3)$ pure gauge theory and in QCD is quite different. Sharp behavior in the former case gives way to smoother change over wide temperature range. The behavior of the Polyakov loop in QCD at low temperatures can be understood in terms of the hadronic degrees of freedom [15, 16]. However, this description breaks down in the vicinity of the transition region.

Another possibility to probe deconfinement is through fluctuations of conserved charges. For instance, light and strange quark number fluctuations, that are suppressed at low temperature,

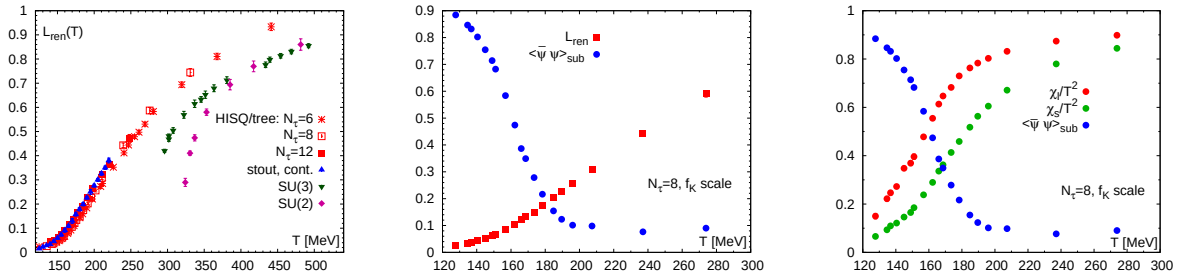

Figure 4. Temperature dependence of the Polyakov loop in $SU(2)$ and $SU(3)$ pure gauge theory and QCD (left). Comparison of the behavior of the renormalized light quark condensate and the Polyakov loop (middle) and light and strange quark number fluctuations (right).

signal liberation of the degrees of freedom with quantum numbers of quarks. In Fig. 4 (middle, right) we compare the light quark condensate to the Polyakov loop, light and strange quark number susceptibility. As one can see, the quantities associated with deconfinement rise somewhat slowly and over substantial temperature range. Thus, deconfinement is a gradual phenomenon in full QCD, and associating a particular temperature with it (by searching for inflection points or alike) does not appear meaningful. Rather, full temperature dependence of various observables should be studied. In particular, one can study fluctuations and correlations of baryon number B, electric charge Q and strangeness S that are given by the derivatives of the pressure with respect to the corresponding chemical potentials

$$\chi_{ijk}^{BQS} = \frac{\partial^{i+j+k}(p/T^4)}{\partial(\mu_B/T)^i \partial(\mu_Q/T)^j \partial(\mu_S/T)^k}. \tag{4}$$

The fluctuations of strangeness, baryon number and electric charge, calculated with the HISQ/tree action and extrapolated to the continuum, are shown in Fig. 5 (HotQCD collaboration [17]). Solid curves represent the Hadron Resonance Gas model, which is in remarkable agreement with the lattice data up to $T \sim 150 - 160$ MeV. (Electric charge fluctuations are the most sensitive to the cutoff effects in the pion sector and obtaining the continuum limit is, thus, a more subtle issue.) The results from the Budapest-Wuppertal collaboration [18] for the same quantities are in complete agreement.

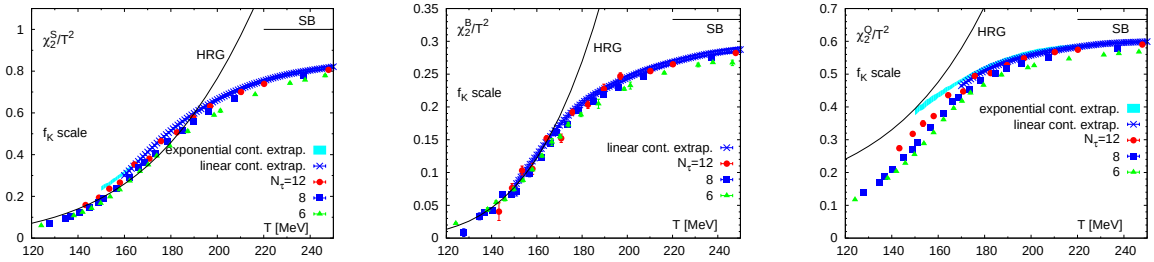

Figure 5. Fluctuations of strangeness, baryon number and net electric charge with the HISQ/tree action extrapolated to the continuum and compared to the Hadron Resonance Gas model.

To probe the critical behavior of QCD further one can consider higher-order cumulants of conserved charges. Comparing ratios of cumulants calculated on the lattice with experimental data, under assumption that at the time of chemical freeze-out the system created in heavy-ion

collisions can be described by equilibrium thermodynamics with temperature T_f and baryon chemical potential μ_B^f, one can extract these freeze-out parameters. A recent attempt to use electric charge fluctuations for this purpose has been presented in Ref. [19]. By constraining the mean net strangeness and electric charge to those of the incident nuclei:

$$M_S = 0, \;\; M_Q = rM_B, \;\; (r \simeq 0.4 \text{ in gold-gold and lead-lead collisions}), \tag{5}$$

one can determine the strange and electric charge chemical potential of the system. To the next-to-leading order (NLO) in the baryon chemical potential:

$$\frac{\mu_Q}{T} = q_1 \, \frac{\mu_B}{T} + q_3 \, \left(\frac{\mu_B}{T}\right)^3, \quad \frac{\mu_S}{T} = s_1 \, \frac{\mu_B}{T} + s_3 \, \left(\frac{\mu_B}{T}\right)^3. \tag{6}$$

The q_i, s_i coefficients are related to ratios of generalized susceptibilities, *i.e.* various combinations of derivatives of the partition function with respect to chemical potentials, Eq. (4). It has been shown in Ref. [19] that NLO corrections are small and at NLO the dependence of μ_Q/μ_B and μ_S/μ_B on μ_B at several temperatures is shown in Fig. 6. The bands give total uncertainty of the lattice calculation and dashed lines represent the HRG model. Once μ_Q and μ_S satisfying the constraint (5) are fixed, ratios of cumulants can be evaluated, and Ref. [19] focused on

$$R_{12}^X \equiv \frac{M_X}{\sigma_X^2} = \frac{\mu_B}{T}\left(R_{12}^{X,1} + R_{12}^{X,3} \, \left(\frac{\mu_B}{T}\right)^2 + \mathcal{O}((\mu_B/T)^4)\right), \tag{7}$$

$$R_{31}^X \equiv \frac{S_X \sigma_X^3}{M_X} = R_{31}^{X,0} + R_{31}^{X,2} \, \left(\frac{\mu_B}{T}\right)^2 + \mathcal{O}((\mu_B/T)^4), \tag{8}$$

where $X = B$ or Q, M_X is mean, σ_X^2 is variance and S_X skewness for corresponding conserved charges. The results are shown in Fig. 7 and 8. If R_{31}^Q is determined from experiment, one can use the band in Fig. 7 to convert it to the freeze-out temperature T_f. Then from an experimentally determined ratio R_{12}^Q, T_f and the corresponding band in Fig. 8 one can find the freeze-out chemical potential μ_B^f. Once the full experimental analysis of R_{31}^Q and R_{12}^Q is available, the results of Ref. [19] can determine T_f and μ_B^f for various center-of-mass energies and thus map a part of the freeze-out curve on the QCD phase diagram.

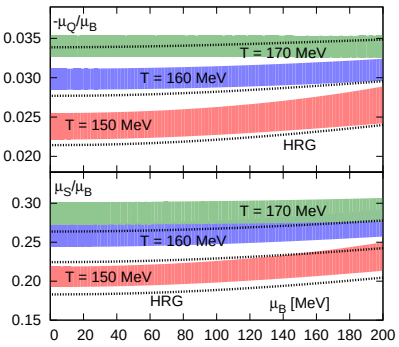

Figure 6. Strangeness and electric charge chemical potential at several temperatures with the constraints (5).

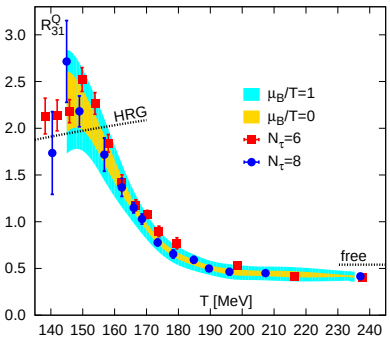

Figure 7. The dependence $R_{31}^Q(T)$ allows for determination of the freeze-out temperature T_f.

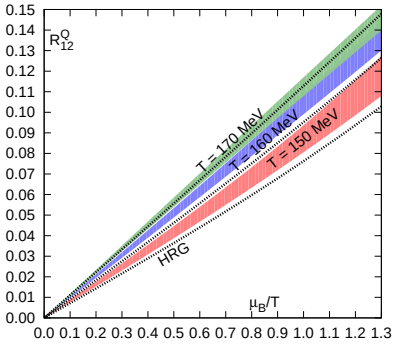

Figure 8. The dependence $R_{12}^Q(T)$ at given T_f determines the freeze-out chemical potential μ_B^f.

4. A list of other results on the lattice

Due to the space constraints many other recent interesting calculations on the lattice could not be included. Among those I would like to mention:

- Progress on the equation of state with 2+1 flavors of staggered fermions: an update of the previous results from the Budapest-Wuppertal [20] and HotQCD [21, 22] Collaboration. Preliminary results still indicate a discrepancy in $150 - 300$ MeV range, which may be resolved by ongoing calculations.
- 2+1 flavor equation of state with Wilson fermions from the WHOT-QCD collaboration [23].
- The equation of state with dynamical charm quark, see Refs. [20] and [24] for preliminary results.
- Calculation of the charmonium screening masses from spatial correlation functions in 2+1 flavor QCD [25] and Maximum Entropy Method (MEM) reconstruction of the charmonium spectral functions in quenched QCD [26].
- Thermodynamics of the crossover region with high magnetic fields [27].

Acknowledgments

I would like to thank the organizers of Hot Quarks 2012 for a very productive and interesting meeting and Frithjof Karsch and Peter Petreczky for careful reading and comments on the manuscript. This work was in part supported by U.S. Department of Energy under Contract No. DE-AC02-98CH10886.

References

[1] Bernard C *et al.* [MILC Collaboration] 2005 *Phys. Rev.* D **71** 034504 (*Preprint* hep-lat/0405029)
[2] Cheng M, Christ N H, Datta S, Van der Heide J *et al.* 2006 *Phys. Rev.* D **74** 054507 (*Preprint* hep-lat/0608013)
[3] Aoki Y, Endrodi G, Fodor Z, Katz S D and Szabo K K 2006 *Nature* **443** 675 (*Preprint* hep-lat/0611014)
[4] Petreczky P 2012 *J. Phys.* G **39** 093002 (*Preprint* 1203.5320)
[5] Pisarski R D and Wilczek F 1984 *Phys. Rev.* D **29** 338
[6] Ejiri S, Karsch F, Laermann E, Miao C *et al.* 2009 *Phys. Rev.* D **80** 094505 (*Preprint* 0909.5122)
[7] Bazavov A, Bhattacharya T, Cheng M, DeTar C *et al.* [HotQCD Collaboration] 2012 *Phys. Rev.* D **85** 054503 (*Preprint* 1111.1710)
[8] Borsanyi S *et al.* [Wuppertal-Budapest Collaboration] 2010 *JHEP* **1009** 073 (*Preprint* 1005.3508)
[9] Bazavov A and Petreczky P 2010 *PoS* **LATTICE2010** 169 (*Preprint* 1012.1257)
[10] Borsanyi S, Durr S, Fodor Z, Hoelbling C *et al.* 2012 *JHEP* **1208** 126 (*Preprint* 1205.0440)
[11] Borsanyi S, Delgado Y, Durr S, Fodor Z *et al.* 2012 *Phys. Lett.* B **713** 342 (*Preprint* 1204.4089)
[12] Bazavov A, Bhattacharya T, Buchoff M I, Cheng M *et al.* [HotQCD Collaboration] 2012 *Phys. Rev.* D **86** 094503 (*Preprint* 1205.3535)
[13] Boyd G, Engels J, Karsch F, Laermann E *et al* 1996 *Nucl. Phys.* B **469** 419 (*Preprint* hep-lat/9602007)
[14] Svetitsky B and Yaffe L G 1982 *Nucl. Phys.* B **210** 423
[15] Megias E, Ruiz Arriola E and Salcedo L L 2012 *Phys. Rev. Lett.* **109** 151601 (*Preprint* 1204.2424)
[16] Bazavov A and Petreczky P 2013 (*Preprint* 1301.3943)
[17] Bazavov A, Bhattacharya T, DeTar C E, Ding H-T *et al.* [HotQCD Collaboration] 2012 *Phys. Rev.* D **86** 034509 (*Preprint* 1203.0784)
[18] Borsanyi S, Fodor Z, Katz S D, Krieg S, Ratti C and Szabo K 2012 *JHEP* **1201**, 138 (*Preprint* 1112.4416)
[19] Bazavov A, Ding H T, Hegde P, Kaczmarek O *et al.* 2012 *Phys. Rev. Lett.* **109** 192302 (*Preprint* 1208.1220)
[20] Borsanyi S, Endrodi G, Fodor Z, Katz S D *et al.* 2011 *PoS* **LATTICE2011** 201 (*Preprint* 1204.0995)
[21] Petreczky P [HotQCD Collaboration] 2012 *PoS* **LATTICE2012** 069 (*Preprint* 1211.1678)
[22] Bazavov A [HotQCD Collaboration] 2012 (*Preprint* 1210.6312)
[23] Umeda T *et al.* [WHOT-QCD Collaboration] 2012 *PoS* **LATTICE2012** 074 (*Preprint* 1212.1215)
[24] Bazavov A *et al.* [MILC Collaboration] 2012 *PoS* **LATTICE2012** 071
[25] Karsch F, Laermann E, Mukherjee S and Petreczky P 2012 *Phys. Rev.* D **85** 114501 (*Preprint* 1203.3770)
[26] Ding H T, Francis A, Kaczmarek O, Karsch F, Satz H and Soeldner W 2012 *Phys. Rev.* D **86** 014509 (*Preprint* 1204.4945)
[27] Bali G S, Bruckmann F, Endrodi G, Fodor Z, Katz S D and Schafer A *Phys. Rev.* D **86** 071502 (*Preprint* 1206.4205)